Sedimentary geomorphology of the Mars Pathfinder landing site

Timothy Jay Parker
Jet Propulsion Laboratory,

James W. Rice, Jr.
Department of Geography, Arizona State University

Abstract. The first landing on Mars in over 20 years will take place July 4, 1997, near the mouth of the Ares Vallis outflow channel located in southeastern Chryse Planitia. Mars Pathfinder, unlike Viking 1, is expected to land on a surface that has a distinct and unambiguous fluvial signature. For safety reasons, the landing site was selected within a broad plains region beyond the mouth of Ares Vallis so as to avoid large topographic obstacles that could pose hazards to the landing. However, this plain is not without its interesting, and in some cases rather problematic, land forms. The 100 km by 200 km landing ellipse contains the following features: (1) primary impact craters, (2) clusters of small secondary craters, (3) streamlined islands, (4) longitudinal grooves, (5) "scabland" or "etched" terrain, (6) pancake-like shields and dike-like structures, (7) knobs or buttes, and (8) a previously undetected, subtle undulating or hummocky texture to the plains surface. The nature of these landforms has important bearing on how we will interpret what we see at the scale of the Pathfinder lander once the first images are transmitted to Earth. With the exception of the craters, all of the remaining features described within the Mars Pathfinder landing ellipse can be interpreted as forming as a result of catastrophic flooding from Ares and Tiu Vanes into Chryse Planitia, either during the flood itself, or through secondary modification of thick flood deposits after the event.

1. Introduction

The Mars Pathfinder landing site (19.5°N, 32.8°W) is located 150 km from the mouth of Ares Vallis (Figure 1). Mars Pathfinder will land 850 km southeast of the Viking 1 Lander (22.5°N, 48"W). Ares Vallis is the easternmost outflow channel of the southern circum-Chryse region. The channel widens in the downstream direction from 25 km to 100 km before debauching into the Chryse basin. The 100 by 200 km landing site ellipse is located on a smooth to gently hummocky plain between large streamlined islands to the south, streamlined islands and knobby terrain to the east, large fresh impact craters (Hamelin, Kin, and Yuty) to the north, and scabland or etched terrain to the west [Parker, 1995; *Golombek et al.,* 1997].

Fig. 1

Catastrophic floods transport massive quantities of sediment and clasts eroded from their source regions and from the terrain in the flood's path. This was the principal motivating factor behind the proposal and selection of this site as a landing site for the Mars Pathfinder spacecraft *[Rice,* 1994; *Kuzmin et al., 1994; Golombek et al., 1997].* Therefore, the Mars Pathtinder lander and its Sojourner microrover should have access to a grab bag of flood-transported rocks from ancient Noachian crustal material, Hesperian ridged plains, and other channel materials [e.g., *Rice and Edgett, 1995; Tanaka, 1995, 1997].*

Ares and Tiu Vanes are among the largest outflow channels on Mars, with calculated flood discharges that were orders of magnitude larger than the Channeled Scabland on Earth [e.g., *Komatsu and Baker,* 1997]. In fact, the landing site is bounded on all sides by channel flow indicators from Ares and Tiu Vanes. Ares Vallis continues as a distinct channel for several hundred kilometers to the north of the landing site, and Tiu Vallis coalesces with flow features from the other large circum-Chryse channels (Simud, Maja, and Kasei Vanes), which then continue beyond the north rim of Chryse basin into Acidalia Planitia [e.g., *Parker et al. 1993].* Several investigators *[Parker et al.,* 1989, *1993; Baker et al., 199 I; Scott et al.,* 1991, 1995] have proposed that the Chryse basin and perhaps even the entire northern plains were once under water (lakes or oceans).

Therefore it would appear that the process of emplacement of surface materials within the landing ellipse should be directly related to the formation of these channels. So why is there even the least confusion about the nature of the surface at the landing site? Shouldn't we expect a fluvial sedimentary deposit? Regardless of the specific channel formation process, whether fluvial, glacial, or debris flow, a number of subsequent processes need to be considered that could have occurred at the site to alter the surface in the more than 1.8 by. since the early Ama-

zonian, when the latest Chryse floods are generally thought to have occurred [e.g., *Scott and Tanaka, 1986; Tanaka,* 1997]. These processes include eolian reworking or burial, permafrost modification, burial by lacustrine or marine sediment, desiccation of wet or icy sediments, and burial by volcanic plains. Permafrost modification and desiccation would have the least effect on the morphology and lithology accessible to the lander, since they involve modification rather than obscuration of the postflood surface. Eolian reworking or burial, lacustrine or marine sediment mantling, or volcanic plains deposits, on the other hand, could drastically affect the kinds of materials available to the Pathfinder science experiments, by partially or completely covering the original catastrophic flood surface. Fortunately, because of the moderate- to high-thermal inertias in this region relative to the Viking 1 landing site (see discussions by *Edgett and Christensen, [1997]), any* eolian or fine lacustrine blanket is not likely to be thick enough to preclude access to surface rocks. Unconsolidated fines (such as eolian deposits) have very low thermal inertias. Similarly, fine-grained lacustrine sediments, even if they are partially cemented, should have low to moderate thermal inertias. Dense bedrock, such as fresh basalt, would exhibit high thermal inertias. The thermal inertia of the landing site would seem to indicate a surface somewhere midway between purely uncemented fines and areally extensive bedrock outcrops.

To complicate efforts further in reconstructing the geologic history of the landing site, even without subsequent modifiers, a catastrophic flood may leave behind fluvial deposits; relatively unmodified, preexisting terrain (in the case of sediment "bypassing" or throughput); or an eroded, preexisting bedrock surface. (The nature of the preexisting surface itself is uncertain. It is reasonable to expect that it may consist of volcanic plains, impact-brecciated megaregolith, or even earlier flood sedimentary deposits). The differences between which of these effects dominate at a given location are determined by the velocity of the flood at the location relative to reaches both in the upstream and downstream directions. High-energy flows will transport sediment through the site or scour the existing surface, whereas a drop in transport energies beyond the mouth of the channel, or within a basin along the path of the flood, will result in net sediment deposition locally. It is usually possible to sort out these various complicating factors at a field locality through careful examination of bed forms and landforms. However, doing so on Mars may require corroborative, high-resolution contextual orbiter images (such as will become available from Mars Global Surveyor after the Pathfinder nominal mission).

The Ares Vallis site has one very important advantage over other potential grab bag sites on Mars that

might be accessible to the spacecraft. Because this site was one of the initial choices for Viking Lander 1, excellent, same-orbit stereo images were acquired early in the Viking mission (Figure l). These stereo pairs are on the order of 40 m/pixel resolution with a separation angle between looks of about 48°, corresponding to a 45 m vertical precision for topographic measurements (based on parallax displacement of a single picture element). Though other stereo pairs are available for this region, the images used in this investigation offer nearly complete coverage of the landing ellipse and have the best separation angle for topographic measurement purposes.

Subtle topography on the plains is most easi ly viewed in stereo and is indispensable to studying the geology of the landing site and surrounding region. It should also prove useful in determining the exact location of the Pathfinder lander on the Martian surface after landing, by providing a correlation between objects viewed on the horizon with a three-dimensional aerial view at least several months before the Mars Global Surveyor Orbiter could image the landing site with the Mars Orbiter Camera (MOC).

We will examine the morphology of the landing site and its immediate surroundings on the basis of Viking Orbiter stereo images, with the goal of offering predictions of what we can expect to see once Pathfinder surface operations begin in July 1997. In general, on the basis of considerations of these landforms, we predict that Pathtinder can expect to find a fluvial sedimentary deposit that has undergone little modification since the latest Chryse flood.

2. Landing Site Morphologies

The landing ellipse contains a number of landforrns, some that are familiar and unequivocal, and some for which the origins are problematic. What do the well-understood landforms tell us about the processes that acted to form them? How does the range of interpretations for the problematic features affect what we anticipate Pathfinder will see?

2.1. Primary Iimpact Craters and Clusters of Small Secondary Craters.

Large, primary craters are relatively few within the landing ellipse (Figure 2). Small, fresh secondary craters (up to 500 m in diameter) are much more abundant and occur in a number of large clusters across the ellipse (Figure 3) [*Greeley et al., 1977; Parker, 1995; Rice, 1995; Golombek et al.*, 1997]. Many of these small craters have dark rims and halos. This may indicate a darker layer underlying the plains that has been excavated by these impacts. *Golombek et al.* [1997] propose that the secondaries originated from a primary source crater to the south,

Fig 2

Fig 3

on the basis of north trending trains with weak fan-like distributions within them, though the candidate crater has not been positively identified.

Impact cratering is, for the most part (at least for the purpose of this discussion), a well-understood process. Crater size-frequency distribution plots can help us determine the age of the surface, in this case late Hesperian to early Amazonian (Figure 4) [*Scott and Tanaka,* 1986; *Tanaka,* 1997]. The potential hazards posed by landing within or near impact craters are discussed in detail elsewhere [*Golombek et al.*, 1997]. In general, however, small craters probably will not pose a serious landing hazard. Landing near, even within, a crater may increase the grab bag potential of a partially buried flood deposit by providing blocks of ejected material.

Fig. 4

2.2, **Streamlined Islands.**

These are large, primary erosional features of the Ares and Tiu Vanes floods (Figure 5) *[Baker,* 1973, 1978]. Streamlined islands can be used to determine the depth of downcutting of preexisting topography by the flood (minus any fill material left behind) and, to a less reliable extent, provide a measure of the maximum possible flood depth (by assuming that the highest water line and lowest channel floor were occupied at the same time). Those within and around the landing site are up to hundreds of meters in height (based on stereo parallax measurements and photoclinometric profiles [*Golombek et al.,* 1997]), several kilometers wide and up to a few tens of ki lometers long. Banding on the flanks of these islands could be due to flood erosion of layered material, cut terraces, till terraces, or combinations of these. Channel terraces could indicate multiple episodes of flooding or multiple stages of downcutting during a single flood.

Fig. 5

A large region of eroded, layered mesas (about 42,000 km^2) is located north-northwest of the Pathfinder landing site (Figure 6). This material has a smooth texture with variable albedo in contrast to the "darker" plains surrounding it. The margins of the material have scalloped erosional scarps, and irregular depressions dot the surface [*Greeley et al.,* 1977]. These mesas are included in a regional unit described as "older channel floor material" (unit Hchh [*Rotto and Tanaka, 1995])* and "Chryse unit 2" by *Tanaka [1997].* The mesas are distributed in an arc concentric to the Chryse basin and may be the erosional remnants of an earlier basin-filling sedimentary deposit. This material is a flat-lying, extensive, layered deposit that was easily eroded by the Ares and Tiu flood(s), resulting in surface pits and scalloped margins with smooth outlines. Though *Rotto and Tanaka [1995]* described this unit as older channel floor material, it is not confined to any recognizable channel, but instead lies well beyond the mouths of the Ares and Tiu Vanes. Since the

Fig. 6

surface of this deposit exhibits no subaerial fan morphology, we suggest that it may be the eroded remnant of an older deltaic or basin-filling lacustrine deposit that records an earlier channel influx into the region during the Hesperian. These mesas also exhibit streamlining on their downstream flanks. The craters Yuty, Wabash, and Wahoo are superposed on this material.

2.3. Longitudinal Grooves,

Longitudinal grooves are also present within the landing ellipse, primarily toward the south and east, generally in association with streamlined islands in those areas (Figures 1 and 5b). Longitudinal grooves can reproduced in relatively high velocity flows in which longitudinal [e.g., *Baker, 1973, 1978]* or "corkscrew" vortices [e.g., *Allen,* 1985] scour the channel bed or construct ridges of sediment parallel to the direction of flow (such as imbricated trains of coarse clasts), through differential sediment deposition *[Allen, 1985].* Longitudinal grooves present within the landing ellipse probably indicate that fluvially transported coarse sediment or channel-scoured bedrock lies at or near the modem surface locally, in order that the morphology not be obscured. However, longitudinal grooving can vary greatly in amplitude, so it is possible that the surface has been mantled bysomelater depositional process, provided that themarrtle is thinner than the total relief on the underlying ridged and grooved surface. Eolian or lacustrine material may drape this surface without obscuring it, but volcanic flows would probably not.

2.4. "Scabland" or Etched Terrain.

Etched terrain lies just west of the landing ellipse (in two areas covering 2600 km^2 and 1800 km^2 [Baker, 1973, 1978]). The etched terrain is associated with flow from Tiu Vallis, not Ares Vallis. This surface (Figure 7) consists of relatively bright, flat-floored depressions on the order of 10-20 m deep (based on photoclinometric profiling [Golombek et al., 1997]) within the locally darker plains surface of Chryse Planitia. Small mesas of the plains can be seen within the etched region, implying that the depressed surface developed through erosion of the formerly continuous plains. Many of the margins of the depressions are straight-sided, though there is no obvious regional structural grain that might correlate with their orientations. The overall orientation of the etched region, roughly north-south in the long dimension, is approximately 45° from that of the local direction of flooding from Tiu Vallis. Other occurrences in this region of less pronounced patches of etched terrain are more intriguing. One notable example in Viking image pair 004A19 and 004A79 has an almost parabolic shape, also oriented about 45" with respect to local channel scour, and therefore

Fig. 7

Fig. 8

probably unrelated to it (Figure 8). The association of this etched surface with the pancake-like shields and dike-like structures (section 2.5) provides some clues as to the timing, if not the mechanism, of formation of this enigmatic terrain.

2.5. Pancake-Like Shields and Dike-Like Structures.

Pancake-1ike shields are very gently sloped to flat-topped circular structures a few kilometers in diameter with little or no obvious relief above the surrounding plains (Figure 9) [*Greeley* et *al.*, 1977; *Hodges and Moore, 1994].* These may have either a lighter or darker albedo than the surrounding plain surface, or they may have a similar albedo, making them hard to delineate at times. The shields are very numerous, often overlapping, and are confined exclusively to the plains (i.e., they do not occur on the streamlined islands or their flanks and tails, though they may be found nearby). Most, though not all, of the pancake-like shields lack obvious central vents (see Figure 9 for exceptions).

Fig. 9

The shields and dikes lack evidence of either channel scour or streamlining despite their large numbers, unlike preflood craters, which commonly show extensive scour on their upstream sides and long debris tails or sheltered preflood surfaces on their lee sides. This suggests the shields and dikes formed after the flood. Furthermore, the etched terrain has developed around the shields and dikes, having preferentially eroded the plains and left many shields standing high on the sides bordering the etched surface and still flush with the surrounding plains, In addition, at least one small crater ejects blanket appears to have locally armored the plains surface (Figure 9a), protecting it from the etching process. These relationships point to etching after flooding and dike emplacement, rather than fluvial plucking during the flood. The etching process must have been capable of removing meters of the surface materials without altering the surface morphology of the plains to either side of the etch pits. Eolian deflation of fine sediment is one possibility but requires that the flood deposits be sand-sized or finer to a depth of 10 or 20 m in the area where the pits are found. Another proposed alternative mechanism might be sublimation of massive ice in the near subsurface after the flood, producing the etch pits through disintegration of ice beneath a thin insulating cover, perhaps a mantle of late stage flood-deposited fines or post flood eolian sediments.

The pancake-like shields and dikes have been interpreted as volcanic structures by *Greeley et al.* [1977] and *Hodges and Moore* [1994]. As such, they may represent a late period of volcanism onto the flood-scoured or flood-deposited surface during the early Amazonian, Though there is no reason volcanic landforms could not be found in a fluvial set-

ting, their occurrence exclusively on the plains surface, never on the flanks or "tails" of streamlined islands, might suggest that they are related in some way to plains sediment deposition, perhaps as pseudovolcanic sedimentary structures, such as sand volcanoes, mud laccoliths, and elastic dikes [e.g., *Li et al., 1996]*. These structures are related to differential loading or seismic lithefaction of rapidly emplaced wet sediments. Though none of these proposed analogs approach the Martian features in size, neither do their depositional settings approach the scale of the Martian outflow channels. The Martian floods were certainly capable of rapidly emplacing thick, wet sediments that could have experienced dewatering on a grand scale after cessation of the flood.

2.6. **Knobs orButtes.**

Knob and buttes are small-scale massifs on the order of several tens of meters (close to the image resolution limit) to 7 km in diameter, but most are less than 1 km in diameter [*Golombek et al.*, 1997]. They are scattered throughout the landing ellipse, though the largest are found on the outwash surface dominated by flow from Tiu Vallis (Figure 10). The knobs may be remnants of resistant rock left behind after the flood [e.g., *Hodges and Moore*, 1994]. However, most show no streamlining, whereas similar-sized streamlined knobs or knobs with prominent lee tails are common throughout the Chryse basin. In addition, many of the knobs occur in clusters, particularly in the lees of the larger streamlined islands (Figure 10a) and regions of flow expansion (Figure 10 b), similar to large boulders within channels but on a scale much too large for familiar modes of transport, as in suspension or as bed load.

Fig. 10

These knobs could be similar to blocks pushed along the bed by terrestrial floods and debris flows. A notable example of this type of transport is found in southern California, where fragments of concrete from the Saint Francis Dam, on the order of thousands of tons in mass, were pushed up to a kilometer downstream when the 47 by 10^6 m^3 reservoir failed catastrophically in 1928 (Figure 11) [e.g., *Outland, 1963]*. Maximum discharges from this flood were from 8 to 9 orders of magnitude smaller than those of the Ares and Tiu Vanes floods [see also *Komatsu and Baker, 1997]*. These blocks were clearly too large to have been transported in suspension or as normal bed load. Instead, they must have slid along the channel bed, perphaps lubricated by the bed load itself (the Sespe Formation, which underlies the portion of the dam that moved downstream, is locally composed of clay-rich distal fan sediments). In a natural terrestrial flood setting, the Dry Falls area of the Channeled Scabland includes a number of very large, intact basalt blocks that were plucked from the cataract and transported several hundred meters downstream (Figure 12).

Fig. 11

Fig. 12

Recently, work by *Masson [1996]* on catastrophic landsliding and debris flow avalanches found along the flanks of the western Canary Islands describes blocks up to 1.2 km across and 200 m high that were carried up to 90 km from the source region. The debris flows contain some blocks that are irregular in shape, and others that are tabular and show evidence of original bedding. Even larger blocks of sediment, up to 5 km across, are found up to 110 km from their source. Inferring a debris flow stage [e.g., *Tanaka, 1995]* during the formation of the circum-Chryse channels may help to explain the origin of the Martian knobs in this region.

2.7. **Undulating or Hummocky Plains Surface.**

Much of the surface of the plains within the landing site ellipse exhibits either a smooth or gently undulating surface. The undulations are most pronounced near the center of the ellipse (Figure 13). This texture became apparent only when the Viking images were contrast-enhanced to bring out subtle details within the plains (typically saturating sunward and shaded slopes of knobs and craters). The plains appear almost rippled, though the rippling is poorly organized and trends with the crests parallel to the flow direction from Tiu Vallis. The wavelengths are on the order of a few kilometers, and amplitudes are up to a few tens of meters (based on a stereo parallax displacement of one pixel or less). Because they are oriented perpendicular to the orientation that true ripple trends associated with Ares or Tiu Vanes might show, they may be hummocks or lobes of sediment that was deposited by the flood, rather than giant current ripples. As such, their mechanism of emplacement, through differential deposition, is similar to that described for deposition of sediment in ridges in grooved terrain (above).

Fig. 13

Figure 1 shows a boundary between longitudinally grooved plains and the smooth and undulating plains. The grooved plains occur in the mouth region of Ares Vanes just south of the landing site ellipse and in the channel east of the landing ellipse. This boundary is gradational where the grooving trends perpendicular to the contact. However, where the grooves trend parallel to the channel margins, particularly adjacent to the streamlined islands to the south (see Figure 5), this contact is sharp. The gradation of the boundary in the downflow direction may mark the change from relatively high velocity flow to the south, with net erosion leaving a surface of scoured bedrock and comparatively thin flood deposits, to a reltively low velocity flow regime to the north, with net deposition leading to a surface dominated by massive sediment accumulation. Alternatively, it has been suggested that this may mark the extent of embayment of the mouth of Ares Vallis by sediment from the Tiu Vallis "debris flow" *[Tanaka, 1997]*. However, because the nature of this bound-

ary across the mouth of Ares Vallis and between coalescing flow features from the two channels is gradational, quite unlike the sharp ramparts characteristic of the edges of debris flows, we infer that both Ares and Tiu Vanes were active at the same time, though flow from the larger Tiu Vallis may have been dominant at the waning stages of flooding (see discussion *of Parker et al., [1993]).*

The three large craters at the north edge of the landing site (Figure 1) may provide a means to measure the thickness of this putative deposit. All three craters exhibit terraces around their inside rims, which are continuous around the insides of the two larger craters. Work on similar crater forms on the moon by *Quaide and Oberbeck [1968]* and *Head [1976],* which they described as "concentric" craters, indicates that concentric terraces form during impact into a target with an unconsolidated surface layer (impact megaregolith on the moon) overlying a cohesive substrate, such as a crystalline bedrock or thick volcanic unit, when the crater diameter is at least several times greater than the depth to the base of the surface layer. This terrace can be at varying depths below the topographic surface beyond the crater rim. On the Moon this depth is a function of the irregularity of the base of the megaregolith *[Head, 1976].* In stereo views of the eastern pair of craters in the Ares Vallis site, the terraces appear to be at roughly the same depth below the plains surface in stereo images, though a simple profile across these two craters (Figure 2) indicates depths from less than a few tens of meters up to more than 200 m below the level of the plains surface surrounding the craters. It is tempting to infer that this level represents a subsurface contact between indurated bedrock, capable of supporting steep crater interior slopes and overlying, unconsolidated flood sediments, which retreated farther from the center of the crater than did the bedrock during formation of the crater cavity. The variation in depth of this interface may reflect buried topography scoured during maximum flood discharge. If the above interpretations are valid, they would seem to indicate a deposit ranging in thickness from O m along the south and east sides of the ellipse, up to a few hundred meters on the north side.

3. Predictions for Mars Pathfinder

Pathfinder should land on a surface somewhat similar to that landed on by Viking 1 over 2 decades ago *[Rice and Edge(t,* 1997; *Edgett and Christensen, 1997],* but probably without bedrock exposures and with a less equivocal fluvial signature. Viking I landed beyond the mouth of Maja Vanes, beyond the last recognizable fluvial bedforms identified in the Viking Orbiter images. The Mars Pathfinder landing site, on the other hand, is clearly within a channel

setting, with Ares and ‘fiu Vanes continuing for hundreds of kilometers beyond the site. Making more specific predictions of the nature of the landing site is risky, since the entire Pathfinder mission will be conducted at a scale from millimeters to tens of me ters (or possibly kilometers, if there are objects on the local horizon) and even catastrophic flood deposits can vary greatly in nature from one locality to the next at those scales. Nevertheless, we predict that Pathfinder will find the landing site to be composed of coarse elastic sediments carried by the Ares and Tiu Vanes floods. Over most of the landing site ellipse, these sediments will be predominantly coarse sands and gravels with disseminated boulders. We do not expect that we will see bedrock exposures at the surface, as this deposit may be tens to even hundreds of meters thick at the center of the landing ellipse. However, large clasts, knobs scattered throughout the ellipse, and blocks of ejects from numerous secondary craters should keep the chances of having accessible rocks in the landing site high.

Subsequent modification of the postflood surface was probably limited to thin or discontinuous, very fine grained subaqueous or eolian mantle deposits. The possible aqueous deposits may have been emplaced at the waning of the flood, when a large lake may have been present in the Chryse basin. Pancake-like shields and etched terrain lie primarily at and beyond the western extreme end of the landing ellipse,\ and are not likely to be present at the actual landing site, unless smaller-scale versions of these structures, not resolved by the Viking Orbiter cameras, are present. Eolian mantles would have begun accumulating after drying of the basin and could be modem.

Acknowledgements. This work was conducted at the Jet Propulsion Laboratory, California Institute of Technology, arrd at the Department of Geography, Arizona State University, under contract with the NASA Planetary Geology and Geophysics Program The authors wish to thank Victor R Baker, Kenneth L. Tanaka, and Matthew P. Golombek for constructive, critical reviews of this work.

T. J. Parker, Jet Propulsion Laboratory, Mail Stop 183-501, 4800 Oak Grove Deive, California Institute of Technology, Pasadena, CA 91109-8099, (tel.: 818-393-1012, fax: 818-393-1 227; e-mail: tparker@jpl.nasa.gov).

JW.Rioce Jr., Department of Geography, Arizona State University, P.O. Box 870104, Tempe, AZ 85287-0104.

(Received November 15, 1996; revised August 5, 1997; accepted August 11, 1997.)

Paper number 97JE02276.
O148-0227/97/97JE-02776$ 09,00

PARKER AND RICE: PATHFINDER LANDING SITE GEOMORPHOLOGY

PARKER AND RICE: PATHFINDER LANDING SITE GEOMORPHOLOGY

PARKER AND RICE: PATHFINDER LANDING SITE GEOMORPHOI.OGY

PARKER AND RICE: PATHFINDER LANDING SITE GEOMORPHOLOGY

PARKER AND RICE: PATHFINDER LANDING SITE GEOMORPHOLOGY

PARKER AND RICE: PATHFINDER LANDING SITE GEOMORPHOLOGY

PARKER AND RICE: PATHFINDER LANDING SITE GEOMORPHOLOGY

PARKER AND RICE: PATHFINDER LANDING SITE GEOMORPHOLOGY

PARKER AND RICE: PATHFINDER LANDING SITE GEOMORPHOLOGY

PARKER AND RICE: PATHFINDER LANDING SITE GEOMORPHOLOGY

PARKER AND RICE: PATHFINDER LANDING SITE GEOMORPHOLOGY

PARKER AND RICE: PATHFINDER LANDING SITE GEOMORPHOLOGY

PARKER AND RICE: PATHFINDER LANDING SITE GEOMORPHOLOGY

PARKER AND RICE: PATHFINDER LANDING SITE GEOMORPHOLOGY

PARKER AND RICE: PATHFINDER LANDING SITE GEOMORPHOLOGY

PARKER AND RICE: PATHFINDER LANDING SITE GEOMORPHOLOGY

PARKER AND RICE: PATHFINDER LANDING SITE GEOMORPHOLOGY

PARKER AND RICE: PATHFINDER LANDING SITE GEOMORPHOLOGY

PARKER AND RICE: PATHFINDER LANDING SITE GEOMORPHOLOGY

PARKER AND RICE: PATHFINDER LANDING SITE GEOMORPHOLOGY

PARKER AND RICE: PATHFINDER LANDING SITE GEOMORPHOLOGY

PARKER AND RICE: PATHFINDER LANDING SITE GEOMORPHOLOGY

PARKER AND RICE: PATHFINDER LANDING SITE GEOMORPHOLOGY

PARKER AND RICE: PATHFINDER LANDING SITE GEOMORPHOLOGY

PARKER AND RICE: PATHFINDER LANDING SITE GEOMORPHOLOGY

PARKER AND RICE: PATHFINDER LANDING SITE GEOMORPHOLOGY

PARKER AND RICE: PATHFINDER LANDING SITE GEOMORPHOLOGY

PARKER AND RICE: PATHFINDER LANDING SITE GEOMORPHOLOGY

PARKER AND RICE: PATHFINDER LANDING SITE GEOMORPHOLOGY

PARKER AND RICE: PATHFINDER LANDING SITE GEOMORPHOLOGY

References

Allen, J. R. L. *Principles of Physical Sedimentology*, 272 pp., Allen and Unwin, Winchester, Mass., 1985,

Baker, V, R., Erosional forms and processes for the catastrophic Pleistocene Missoula Floods in eastern Washington, in *Publications in Geomorphology*, edited by M, Morisawa, pp. *123-148,* State Univ. of New York, Binghamton, NY., 1973,

Baker, V, R.. Large-scale erosional and depositions features of the Channeled Scabland, in *The Channeled Scabland,* edited by V. R. Baker and D. Nummedal, pp. 81-115, Planet. Geol. Program, NASA Off. of Space Sci., Washington, D. C., 1978.

Baker, V. R., R. G. Strom, V. C. Gulick, J. S. Kargel, G. Komatsu, and V. S. Kale, Ancient oceans, ice sheets and the hydrological cycle of Mars, *Nature,* 352, 589-594, 1991.

Edgett, K. S., and P. R Christensen, Reeks and eolian features in the Mars Pathfinder landing site region: Viking infrared thermal mapper observations, *J. Geophys. Res.,* 102,4107-4116, 1997.

Golombek, M. P., R A. Cook, H. J. Moore, and T. J. Parker, Selection of the Mars Pathfinder landing site, *J. Geophys. Res.,* 102,3967-3988, 1997.

Greeley, R., E. Theilig, J. E, Guest, M. H. Carr, H. Masursky, and J. A. Cutts, Geology of Chryse Planitia, *J. Geophys. Res.,* 82,4093-4109, 1977.

Head, J. W., The significance of substrate characteristics in determining morphology and morphometry of lunar craters, *Proc. Lunar Sci. Conf., 7th, 2913-2929, 1976.*

Hodges, C. A., and H. J. Moore, Atlas of volcanic landforms on Mars, *U, S. Geol. Surv. Prof. Pap., 1534, 194* pp., 1994.

Howington-Kraus, E., R L, Kirk, B. Redding, and L. A. Soderblom, High-resolution topographic map of the Ares Tiu landing site from Viking Orbiter data, in Mars *Pathfinder Landing Site Workshop II: Characteristics of the Ares Vallis Region and Field Trips in the Channeled Scabland, Washington,* edoted bu M. P. Golombek, K. S. Edgett and J. W. Rice Jr., *LPI Tech, Rep. 95-01,* part *2,* pp. 39-40, Lunar and Planet, Inst., Houston, Tex., 1995.

Komatsu, G., and V. R Baker, Paleohydrology and flood geomorphology of Ares Vallis. *J. Geophys. Res., 102, 4151-4160, 1997.*

Kuzmin, R. O., R. Landheim, and R. Greeley, Potential tanding sites for Mars Pathfinder, in Mars *Pathfinder Landing Site Workshop,* edited by M. P. Golombek, *LPI Tech. Rep. 94-04,* pp. *30-3 t,* Lunar and Planet. Inst., Houston, Tex., 1994,

Li, Y., J. Craven, E. S. Schweig, and S. F. Obermeier, Sand boils induced by the 1993 Mississippi River flood: Could they one day be misinterpreted as earthquake-induced liquefaction?, *Geology,* 24, 171-174, 1996.

Masson, D. G., Catastrophic collapse of the volcanic island of Hierro 15 ka ago and the history of landslides in the Canary Islands, *Geology,* 24, 231-234, 1996.

Outland, C. F., *Man-Made Disaster; The Story of St. Francis Dam, 249* pp., Arthur H. Clark, Glendale, Calif., 1963.

Parker, T. J., Viking stereo of the Ares Vallis site: Sedimentological impl i cat ions, in Mars *Pathfinder Landing Site Workshop II: Characteristics of the Ares Vallis Region and Field Trips in the Channeled Scabland, Washing/on,* edited by M. P. Golombek, K. S. Edgett, and J. W. Rice Jr., *LPI Tech. Rep. 95-01,* part 1, pp. *23-24,* Lunar and Planet. hrst, Houston, Tex., 1995.

Parker, T. J., R. S. Saunders, and D. M. Schneeberger, Transitional morphology in west Deuteronilus Mensae,

Mars: Implications for modification of the lowland/upland boundary, *Icarus,* 82, 111-135, 1989,

Parker, T. J., D. S. Gorsline, R. S. Saunders, D. C. Pieri, and D. M. Schneeberger, Coastal geomorphology of the Martian Northern Plains, *J. Geophys. Res.,* 98, 11,061-11,078, 1993.

Quaide, W. L., and V. R. Oberbeck, Thickness determinations of the lunar surface layer from lunar impact craters, *J. Geophys. Res.,* 73, 5247-5270, 1968.

Rice, J. W., Jr., Maja Vanes and the Chryse outflow complex sites, in Mars *Pathfinder Landing* Site *Workshop,* edited by M. P. Golombek, *LPI Tech. Rep. 94-04,* p. 36, Lunar and Planet. Inst., Houston, Tex., 1994.

Rice, J. W., Jr., The geologic mapping of the Ares Vallis Region, in Mars *Pathfinder Landing Site Workshop II: Characteristics of the Ares Vallis Region and Field Trips m the Channeled Scabland, Washington,* edited by M. P. Golombek, K. S. Edgett, and J. W. Rice Jr., *LPI Tech. Rep, 95-01,* part 1, p. *24,* Lunar and Planet. Inst., Houston, Tex., 1995.

Rice, J. W., Jr., and K. S. Edgett, Catastrophic flood sediments in Chryse Basin, Mars, and Quincy Basin, Washington: Application of sandar facies model, *J. Geophys. Res.,* 102,41854200, 1977.

Rice, J. W., Jr., and K. S. Edgett, A sojourner's prospectus: Provenance of flood-transported clasts at the Mars Pathfinder landing site, in Mars *Pathfinder Larding Site Workshop II: Characteristics of the Ares Vallis Region and Field Trips in the Channeled Scabland, Washington,* edited by M. P. Golombek, K. S. Edgett, and J. W. Rice Jr., *LPI Tech. Rep. 95-01,* part 1, pp. *25-26,* Lunar and Planet. Inst., Houston, Tex., 1995.

Rotto, S., and K. L. Tanaka, Geologic/geomorphic map of the Chryse Planitia region of Mars, irr *Chryse Planitia, Atlas of Mars Geol. Ser., U.S. Gee. Sur. Misc. Invest. Ser. Map, I-2441,* 1995.

Scott, D. H., and Tanaka, K. L. Geologic map of the western equatorial region of Mars, in *Atlas of Mars Geol.* Ser., scale 1:15,000,000, *U.S. Geol. Sur. Misc. Invest. Ser. Map, I-1802-A, 1995.*

Scott, D. H., J. W. Rice Jr., and J. M. Dohm, Martian paleolakes and waterways: Exobiologic implications, *Origin Life Evol. Biosphere, 21,* 189-198, *1991.*

Scott, D. H., J. M. Dohm, and J. W. Rice, Jr., Map showing channels and possible paleolake basins, *U.S. Geol Surv. Misc. Invest. Ser. Map, I-2461,* 1995.

Tanaka, K. L., The stratigraphy of Mars, *Proc. Lunar Planet. Sci. Conf. 17th,* part 1, in *J. Geophys. Res., 91,* Suppl., El 39-El 58, 1986.

Tanaka, K, L., Geologic history of Chryse Planitia, Mars, in Mars *Pathfinder Landing Site Workshop 1[: Characteristics of the Ares Vallis Region and Field Trips in the Channeled Scabland, Washington,* edited by M. P. Golombek, K. S. Edgett, and J. W. Rice Jr., *LPI Tech. Rep. 95-01,* part *2,* pp. 39-40, Lunar and Planet. Inst., Houston, Tex., 1995.

Tanaka, K. L,., Sedimentary history arrd mass flow structures of Chryse and Acidalia Planitiae, Mars, *J. Geophys. Res., 102, 4131-4149,* 1997.

FIGURE CAPTIONS

Figure 1. Mars Pathfinder Ares Vallis landing site. The landing ellipse is [00 by 200 km in size, centered at 19.5° lat.\ itude, 32.8° longtitude. North is toward top of frame. The location of stereo image coverage of the site from orbit O04A, Viking Orbiter 1, is outlined by short-dashed line. Subsequent figures are indicated by numbered boxes. Black arrows indicate flow from Tiu Vallis. White arrows indicate flow from Ares Vallis. The limit of longitudinal grooves is indicated by the long-dashed line.

Figure 2. Stereo pair of fluidized ejects craters north of the Pathfinder landing site. The crater at left, Hamelin, is 8-10 km in diameter and over 600 m deep. The crater at right is only 4 km in diameter and still over 700 m deep. The stereo parallax measurements of these craters reveal an internal terrace up to 200 m below the level of the surrounding plains. This terrace may represent a material difference, possibly a subsurface contact between bedrock at depth overlain by unconsolidated flood sediments and crater ejects profile (bottom) is from Viking Orbiter images (let?) 004A30, 32 and (right) 004A90. The profile is compiled from simple parallax displacement images. Regional tilt due to imprecision in image map projections was removed by subtracting a simple line fit to the original data. Elevations within profile are relative. However, the profile was fit to the elevation of crater rim crests derived by *Howington-Kraus, et al. [1995]* for comparison purposes.

Figure 3. Stereo pair of secondary crater field near center of Pathfinder landing site ellipse, from Viking Orbiter images (left) 004A28 and (right) 004A88.

Figure 4. Cumulative crater size-frequency distribution for the Ares Vallis landing site ellipse, with Martian epochs for age comparisons (adapted from Tanaka, [1986]).

Figure 5. (a) Streamlined islands and longitudinal grooves at south edge of Pathfinder landing site ellipse. The streamlined tail of this island is approximately 250 m in maximum height. Divide crossings are indicated by "D" and formed when flood waters spilled over the island and carved out a linear channel with flat floors and steep walls, or widened and deepened preexisting gaps. Divide crossings help establish the lower limits for the high water surface elevation. From Viking Orbiter images 004A23 (left) and O04A83 (right). (b) A field of longitudinal grooves, parallel to flow direction from Ares Vallis, covering an expanse of 140 km long by 45 km wide. These grooves are found about 50 km east of the Mars Pathfinder landing ellipse. Individual grooves are tens of kilometers long and have spacings of 100-300 m. The largest craters in the image field are I km in diameter. Viking Orbiter image 003A58.

Figure 6. (a) Possible dissected deltaic or lacustrine material indicating an earlier period of sedimentation in the region. At this scale the material has a smooth texture with variable albedo in contrast to the darker floodplains surface. Irregular scalloped scarps form the margins of the deposit. Note the streamlining along the downstream flanks of the deposit (arrows). The crater Yuty (18 km in diameter) is the freshest crater, with multiple ejects lobes, superposed on the deposit. Viking Orbiter image 827A24. (b) Stereo image pair showing layering exposed near eroded margin of deposit. At this scale a number of scattered, shallow pits can be seen in the surface of the deposit. See Figure 6a for location. Viking Orbiter images (left) O08A87 and (right) 034A81.

Figure 7. Scabland, or etched terrain, in plains southwest of Pathfinder landing site ellipse. The darker surface is uneroded plains material. The brighter surface is the base of the etching or scab surface. From Viking Orbiter images (left) 004A20, 22 and (right) O04A80, 82.

Figure 8. Unusual, parabola-shaped etched terrain in plains southwest of Pathfinder landing site ellipse. Darker surface is uneroded plains material. Brighter surface is base of etching or scab surface. From Viking Orbiter images (left) 004A 19 and (right) 004A79 (the bottom of the right image is not in stereo (gap till from 004a19).

Figure 9. Examples of pancake-like shields and dikes west of landing site ellipse. Shields and dikes may be either lighter, darker, or comparable in albedo to surrounding plains surface. (a) Bright shields and dikes against dark plains. Crater ejects blanket (below center of scene) appears to have armored the plains surface, protecting from the etching process. From Viking Orbiter frames (let?) 004A 19 and (right) 004A79. (b) A 4-km-diameter shield at edge of etched terrain. The albedo of shield is only slightly darker than that of surrounding plains, making its outline nearly invisible. From Viking Orbiter frames (left) 004A16 and (right) 004A76. (c) Dark shield surrounded completely by etched plains. From Viking Orbiter frames (left) 004A22 and (right) 004A82. Possible central vents are detectable on some of these shields. The 5-km bright shield in Figure 9a has a low mound near its center (partly overlapped by small impact crater). The 4-km shield in Figure 9b has faint, slightly darker circular feature at its center. Shield at top left in Figure 9C has a small knob, possibly a plug, at its center.

Figure 10. (a) Small knobs or "blocks" on lee side of streamlined island shown in Figure 5. Flow from Ares Vallis was from the bottom of the scene. Flow from Tiu Vanes was around either side of the island at the left of the scene. From Viking Orbiter flames (left) 004A25 and (right) 004A85. (b) "Block field" northwest of landing ellipse where flow from Tiu Vallis expanded rapidly. The largest blocks, denoted

by "A", are nearly 0.5 km in diameter. Viking Orbiter image O03A06.

Figure 11. Saint Francis Dam, Southern California. (a) Aerial photomosaic of the dam, part of the reservoir, and canyon just downstream from the reservoir, taken after the dam failure in March 1928. (b) Enlarged view of the mosaic in Figure I I a, showing dam ("D') and reservoir ("R') locations as well as the locations of Figures 11 c and 11 d (also outlined, but not labeled, in Figure 1 la).. (c) Stereo photo pair of the largest dam fragments transported over 0.6 km from the dam site. (d) Stereo photo pair of a second group of large dam fragments transported up to 1 km from the dam site. Aerial photographs courtesy Fairchild Aerial Photography Collection, Whittier College Geology Department.

Figure 12. Dry Falls Cataract, Channeled Scabland, Washington. (a) A 180° panorama photomosaic of Dry Falls from cataract and scour pools at left, to block-strewn field downstream at right. (b) Enlargement of area outlined in Figure 12a, showing block-strewn field. Note dirt road for scale.

Figure 13. Undulating plains surface texture in landing site ellipse. Flow direction from Tiu Vallis was from left to right across the scene (see also Figure 3 for continuation of this surface and texture into secondary crater field to east). These undulations are repeated in the same position relative to surface features from one image to the next (not relative to the image frames) and exhibit relief in stereo views, and so are true landforms rather than image artifacts. Viking Orbiter images (left) O04A28; (right) O04A88; see also O04A86.

Figure 1. Mars Pathfinder Ares Vallis landing site. The landing ellipse is 100 by 200 km in size, centered at 19.5° lat.\itude, 32.8" longtitude. North is toward top of frame. The location of stereo image coverage of the site from orbit 004A, Viking Orbiter 1, is outlined by short-dashed line. Subsequent figures are indicated by numbered boxes. Black arrows indicate flow from Tiu Vallis. White arrows indicate flow from Ares Vallis. The limit of longitudinal grooves is indicated by the long-dashed line.

Figure 2. (top) Stereo pair of fluidized ejects craters north of the Pathfinder landing site. The crater at left, Hamelin, is 8-10 km in diameter and over 600 m deep. The crater at right is only 4 km in diameter and still over 700 m deep. The stereo parallax measurements of these craters reveal an internal terrace up to 200 m below the level of the surrounding plains. This terrace may represent a material difference, possibly a subsurface contact between bedrock at depth overlain by unconsolidated flood sediments and crater ejects profile is from Viking Orbiter images (left) 004A30, 32 and (right) 004A90. (bottom) The profile is compiled from simple parallax displacement images. Regional t i It due to imprecision in image map projections was removed by subtracting a simple line fit to the original data. Elevations within profile are relative. However, the profile was fit to the elevation of crater rim crests derived by *Hewing/on-Kraus, et al. [1995]* for comparison purposes.

Figure 3. Stereo pair of secondary crater field near center of Pathfinder landing site ellipse, from Viking Orbiter images (left) 004A28 and (right) 004A88.

Figure 4. Cumulative crater size-frequency distribution for the Ares Vallis landing site ellipse, with Martian epochs for age comparisons (adapted from *Tanaka, [1986]).*

Figure 5. (a) Streamlined islands and longitudinal grooves at south edge of Pathfinder landing site ellipse. The streamlined tail of this island is approximately 250 m in maximum height. Divide crossings are indicated by "D' and formed when flood waters spilled over the island and carved out a linear channel with flat floors and steep walls, or widened and deepened preexisting gaps. Divide crossings help establish the lower limits for the high water surface elevation. From Viking Orbiter images 004A23 (left) and 004A83 (right). (b) A field of longitudinal grooves, parallel to flow direction from Ares Vallis, covering an expanse of 140 km long by 45 km wide. These grooves are found about 50 km east of the Mars Pathfinder landing ellipse. Individual grooves are tens of kilometers long and have spacings of 100-300 m. The largest craters in the image field are 1 km in diameter. Viking Orbiter image 003A58.

Figure 6. (a) Possible dissected deltaic or lacustrine material indicating an earlier period of sedimentation in the region. At this scale the material has a smooth texture with variable albedo in contrast to the darker floodplains surface. Irregular scalloped scarps form the margins of the deposit. Note the streamlining along the downstream flanks of the deposit (arrows). The crater Yuty (18 km in diameter) is the freshest crater, with multiple ejects lobes, superposed on the deposit, Viking Orbiter image 827A24. (b) Stereo image pair showing layering exposed near eroded margin of deposit. At this scale a number of scattered, shallow pits can be seen in the surface of the deposit. See Figure 6a for location. Viking Orbiter images (left) 008A87 and (right) 034A81.

Figure 7. Scabland, or etched terrain, in plains southwest of Pathfinder landing site ellipse. The darker surface is uneroded plains material. The brighter surface is the base of the etching or scab surface. From Viking Orbiter images (left) 004A20, 22 and (right) 004A80, 82.

Figure 8. Unusual, parabola-shaped etched terrain in plains southwest of Pathfinder landing site ellipse. Darker surface is uneroded plains material, Brighter surface is base of etching or scab surface. From Viking Orbiter images (left) 004A 19 and (right) 004A79 (the bottom of the right image is not in stereo (gap fill from 004a19).

Figure 9. Examples of pancake-like shields and dikes west of landing site ellipse. Shields and dikes may be either lighter, darker, or comparable in albedo to surrounding plains surface. (a) Bright shields and dikes against dark plains. Crater ejects blanket (below center of scene) appears to have armored the plains surface, protecting from the etching process. From Viking Orbiter frames (left) 004A 19 and (right) O04A79. (b) A 4-km-diameter shield at edge of etched terrain. The albedo of shield is only slightly darker than that of surrounding plains, making its outline nearly invisible. From Viking Orbiter frames (left) O04A 16 and (right) O04A76. (c) Dark shield surrounded completely by etched plains. From Viking Orbiter frames (left) 004A22 and (right) O04A82. Possible central vents are detectable on some of these shields, The 5-km bright shield in Figure 9a has a 10 w mound near its center (partly overlapped by small impact crater). The 4-km shield in Figure 9b has faint, slightly darker circular feature at its center. Shield at top left in Figure 9c has a small knob, possibly a plug, at its center.

Figure 10. (a) Small knobs or "blocks" on lee side of streamlined island shown in Figure 5. Flow from Ares Vallis was from the bottom of the scene. Flow from Tiu Vanes was around either side of the island at the left of the scene. From Viking Orbiter frames (left) 004A25 and (right) 004A85. (b) "Block field" northwest of landing ellipse where flow from Tiu Vallis expanded rapidly. The largest blocks, denoted by "A", are nearly 0.5 km in diameter. Viking Orbiter image 003A06.

Figure 11. Saint Francis Darn, Southern California, (a) Aerial photomosaic of the dam, part of the reservoir, and canyon just downstream from the reservoir, taken after the darn failure in March 1928.

(b) Enlarged view of the mosaic in Figure 1 la, showing dam ("D") and reservoir ("R') locations as well as the locations of Figures I lc and 1 ld (also outlined, but not labeled, in Figure 1 la).. (c) Stereo photo pair of the largest dam fragments transported over 0.6 km from the dam site. (d) Stereo photo pair of a second group of large darn fragments transported up to 1 km from the dam site. Aerial photographs courtesy Fairchild Aerial Photography Collection, Whittier College Geology Department.

Figure 12. Dry Falls Cataract, Channeled Scabland, Washington. (a) A 180° panorama photomosaic of Dry Falls from cataract and scour pools at left, to block-strewn field downstream at right. (b) Enlargement of area outlined in Figure 12a, showing block-strewn field. Note dirt road for scale.

Figure 13. Undulating plains surface texture in landing site ellipse. Flow direction from Tiu Vallis was from left to right across the scene (see also Figure 3 for continuation of this surface and texture into secondary crater field to east). These undulations are repeated in the same position relative to surface features from one image to the next (not relative to the image frames) and exhibit relief in stereo views, and so are true landforms rather than image artifacts. Viking Orbiter images (left) 004A28; (right) 004A88; see also 004A86.

Figure 5. (continued)

Figure 6. (continued)

Figure 9. (continued)

Figure 10. (continued)

Figure 11. (continued)

Figure 1 I. (continued)

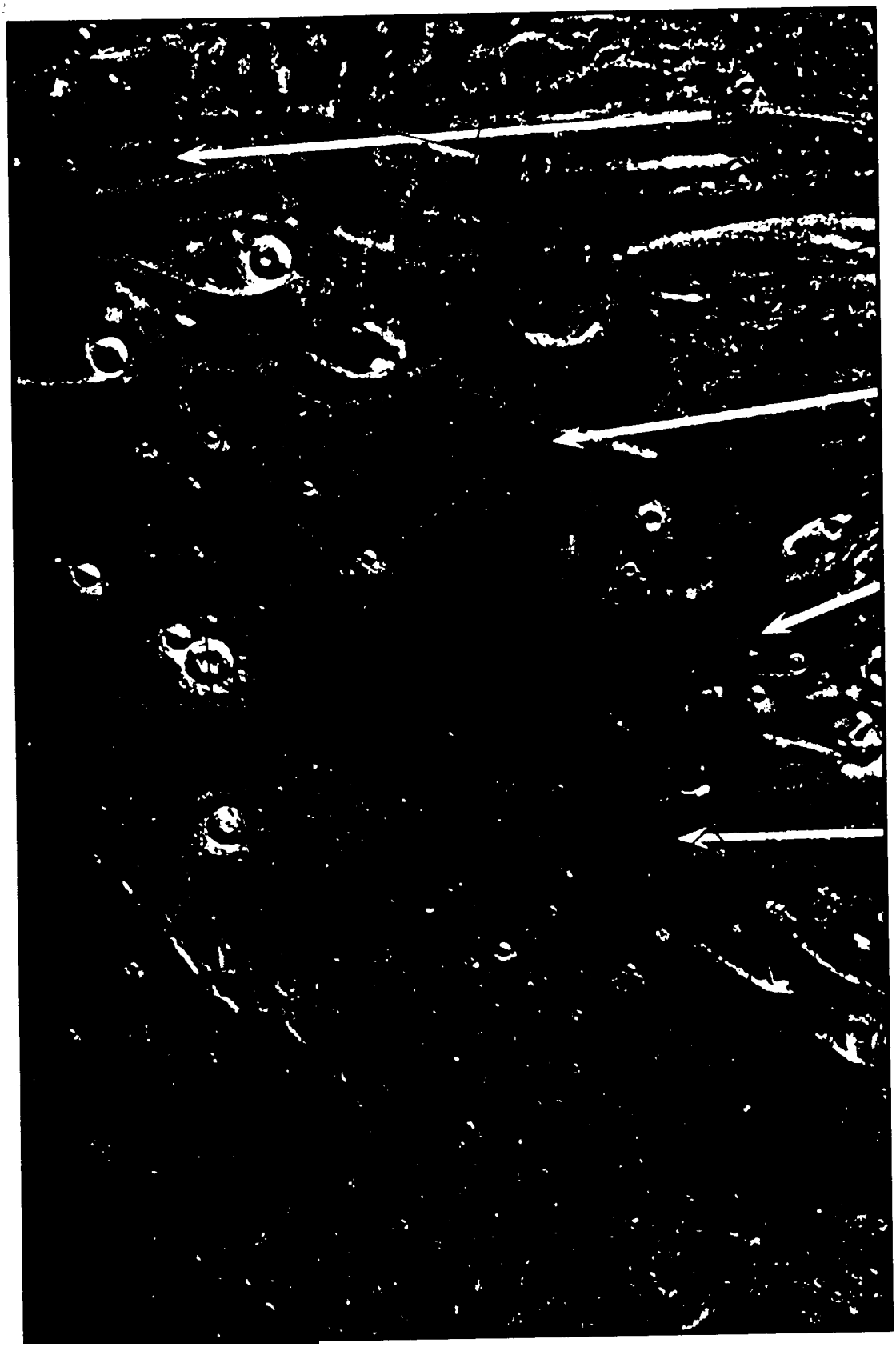

Fig. 1

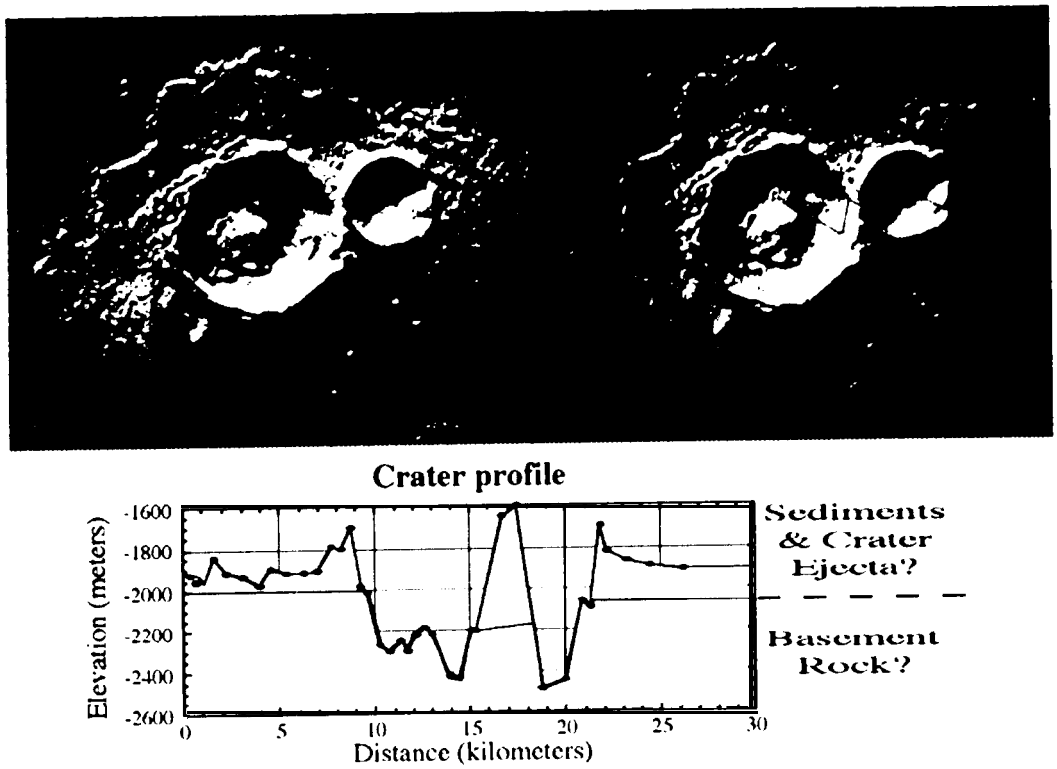
Crater profile
Elevation (meters)
-1600
-1800
-2000
-2200
-2400
-2600
0
5
10
15
20
25
30
Distance (kilometers)
Sediments & Crater Ejecta?
Basement Rock?

Fig. 2

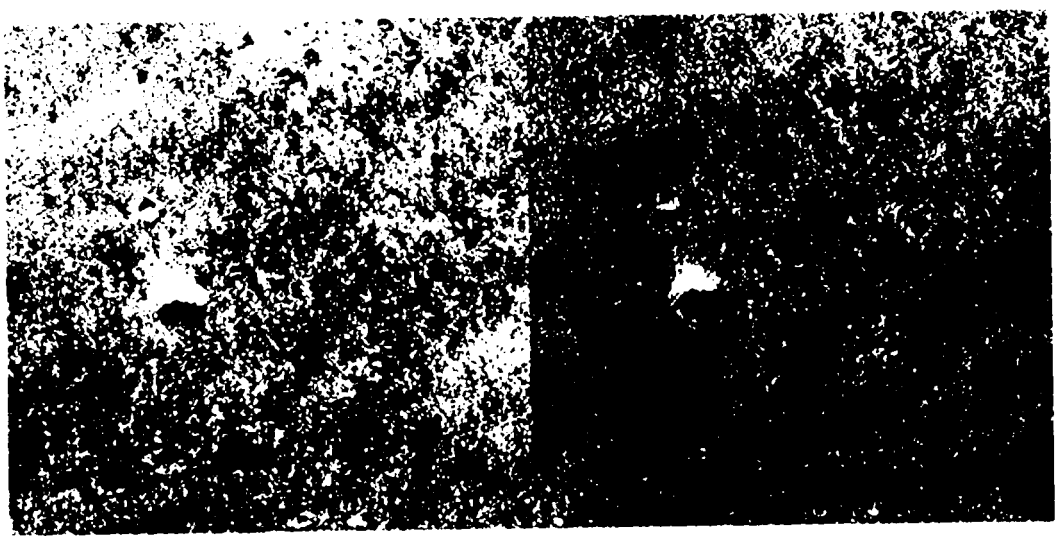

Fig. 3

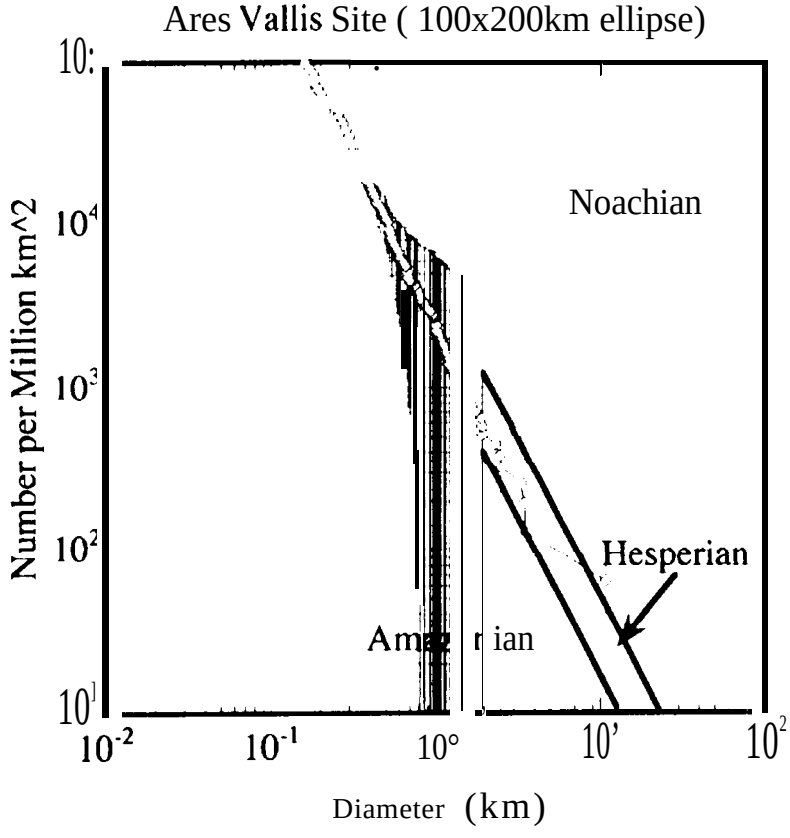
Ares Vallis Site (100x200km ellipse)
Number per Million km^2
Noachian
Hesperian
Amazonian
Diameter (km)

Fig. 4

Fig. 5a

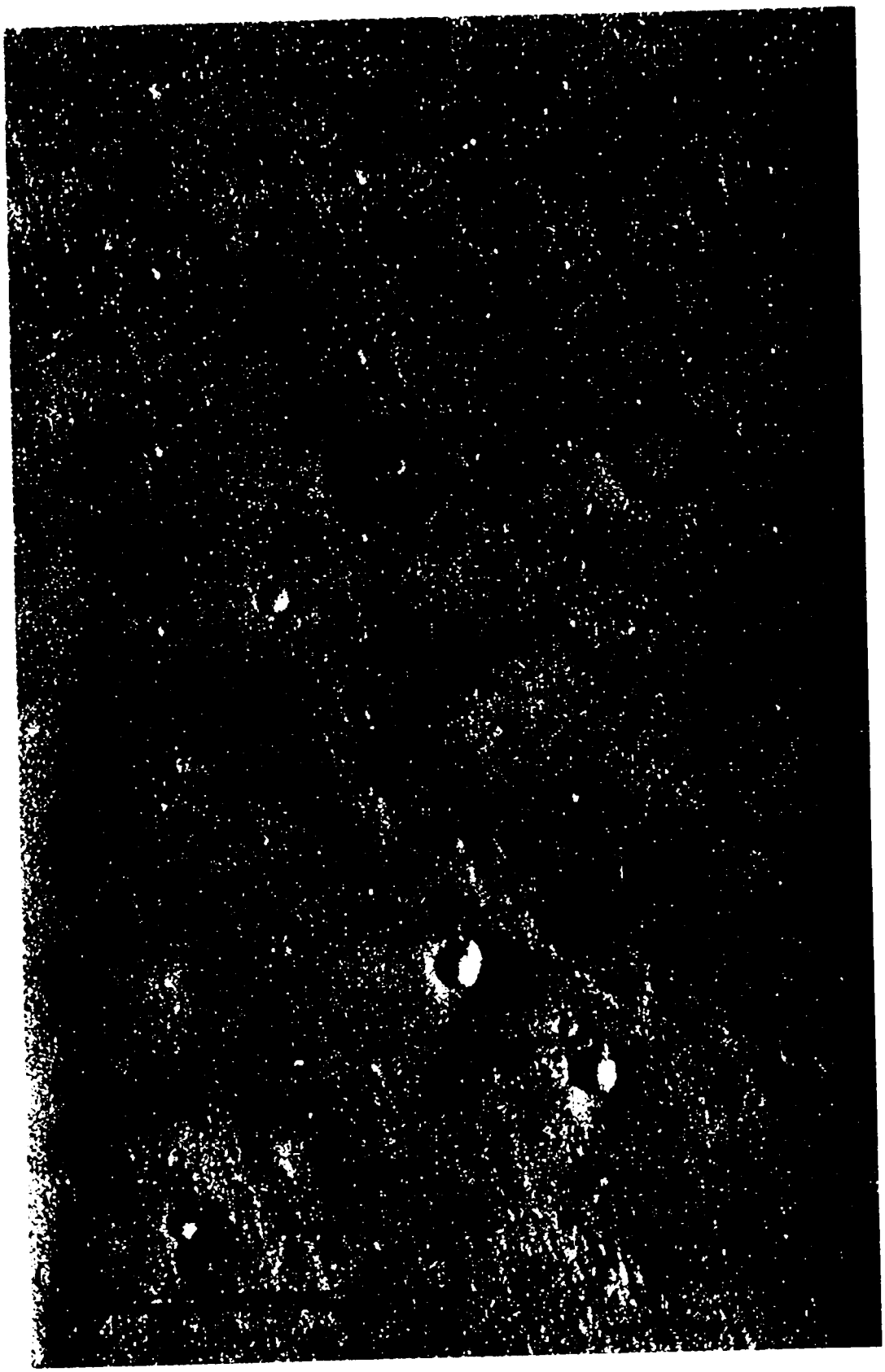

Fig. 5b

Fig. 6a

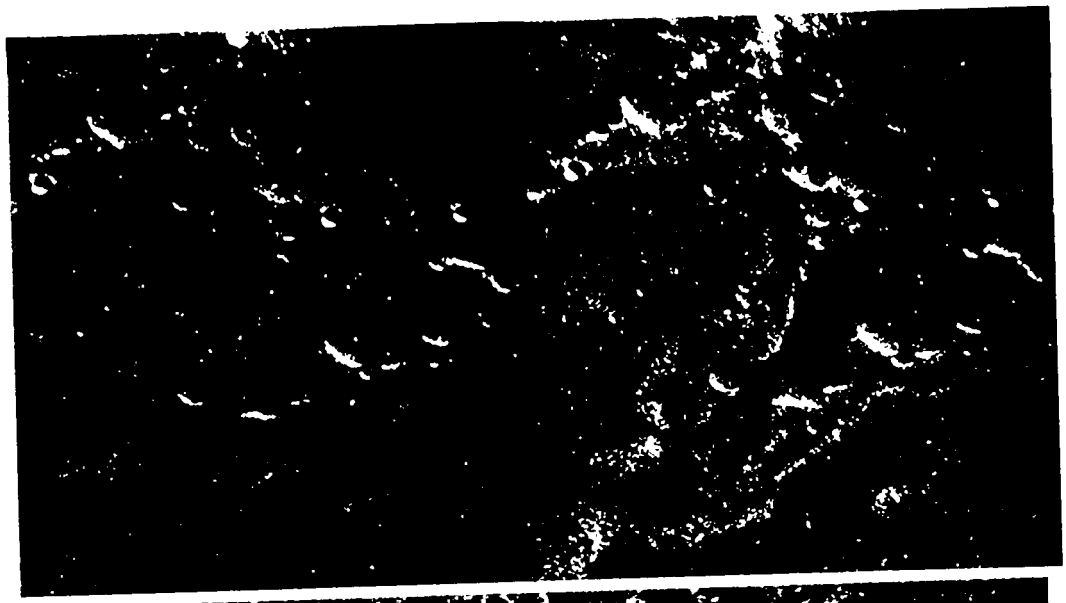

Fig. 6b

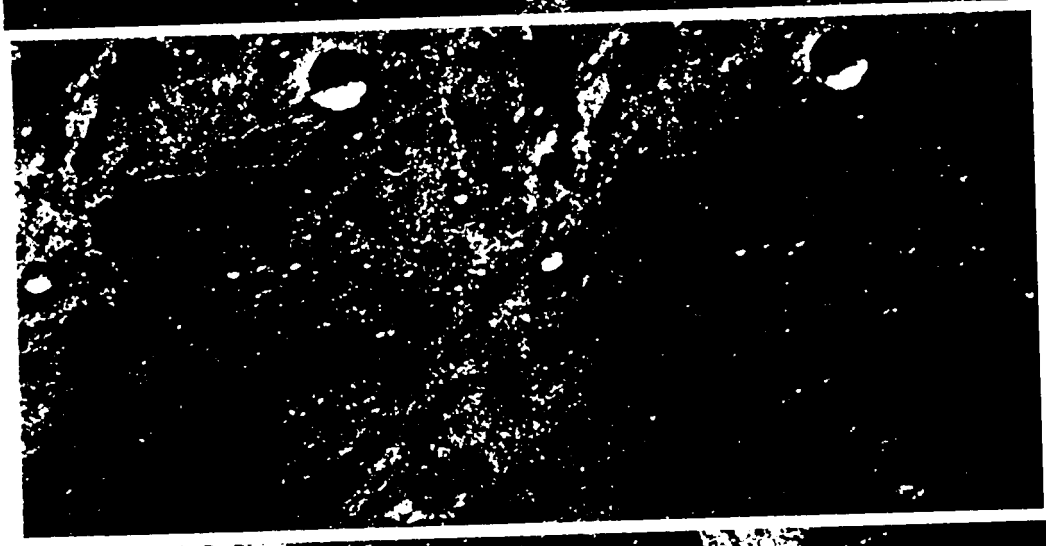

Fig. 7

Fig. 8

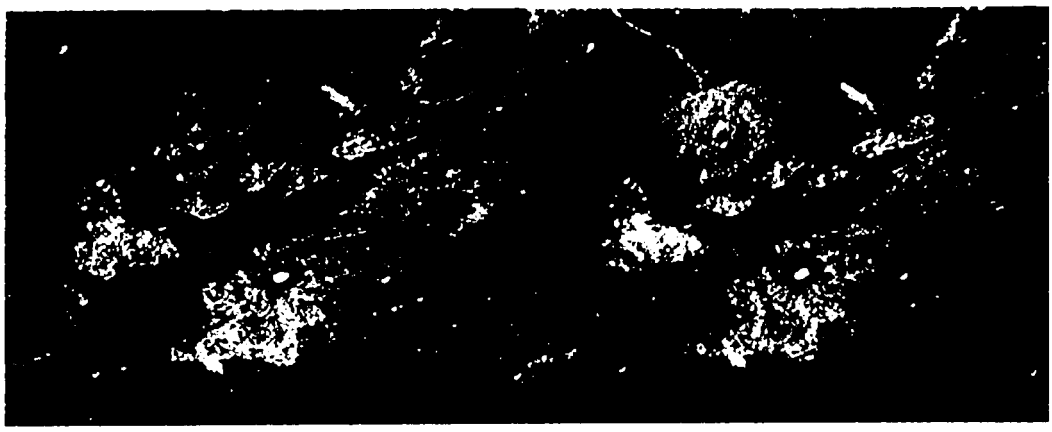

Fig. 9a

Fig. 9b

Fig. 9c

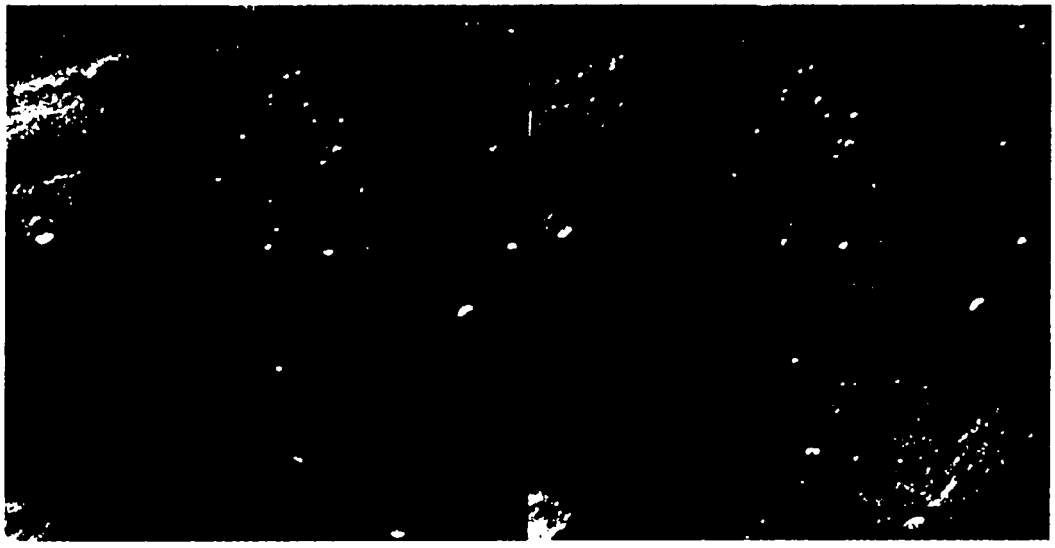

Fig. 10a

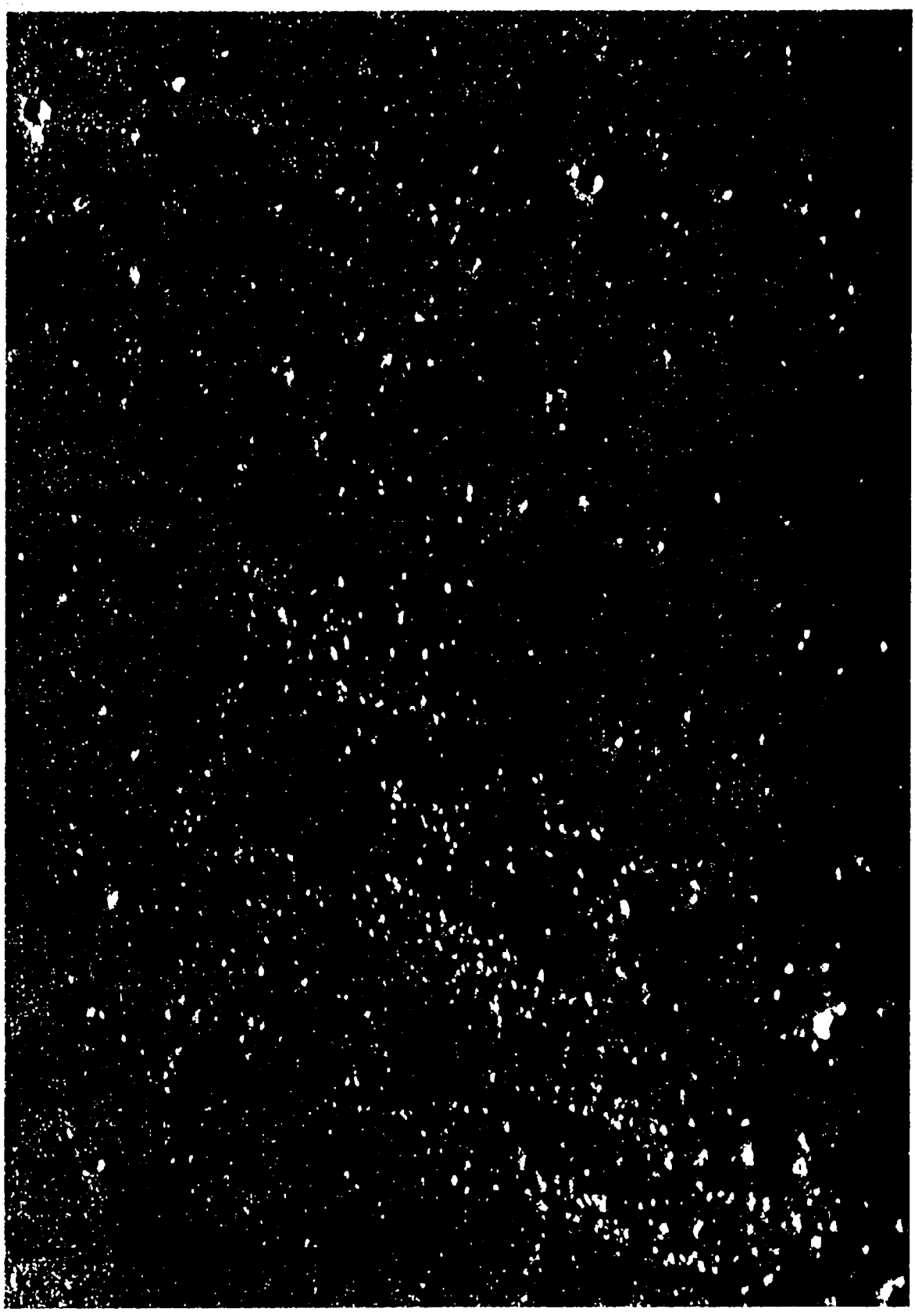

Fig. 10b

Fig. 1a

b

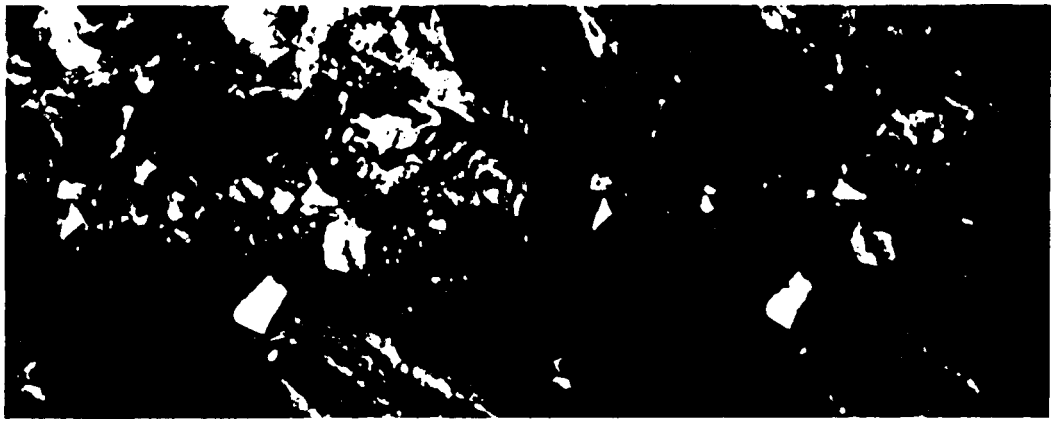

Fg

Fg

Fig. 12

Fig. 13